Fluorescence Resonance Energy Transfer in Novel Multiphoton Absorbing Dendritic Structures†

Darryl W. Brousmiche, Jason M. Serin, and Jean M. J. Fréchet*

Department of Chemistry, University of California, Berkeley, California, 94720-1460 and Materials Sciences Division, Lawrence Berkeley National Laboratory, Berkeley, California 94720

Guang S. He, Tzu-Chau Lin, Sung-Jae Chung, and Paras N. Prasad*

Institute for Lasers, Photonics and Biophotonics, State University of New York at Buffalo, Buffalo, New York 14260-3000

Ramamurthi Kannan and Loon-Seng Tan*

Polymer Branch, AFRL/MLBP, 2941 P St, Suite 136, Area B, Building 654, Wright-Patterson AFB, Ohio 45433-7750

Received: January 6, 2004; In Final Form: March 5, 2004

A series of small dendritic structures containing one of two efficient multiphoton absorbing dyes at the periphery and a nile red derivative at the core have been synthesized. These molecules display efficient (>96%) fluorescence resonance energy transfer (FRET) from the periphery to the core on selective excitation of the two-photon absorbing chromophore by either UV (linear absorption) or high-intensity IR (nonlinear absorption) radiation. In addition, a significant increase in core emission is observed on excitation of the peripheral chromophores, compared to direct excitation of the core. This "antenna effect" essentially doubles between increasing dendrimer generations within a series. The combination of the ability of the peripheral chromophores to absorb high-intensity IR radiation, coupled with a very efficient energy transfer process and a significant increase in the fluorescence of the acceptor chromophore, makes these molecules potentially useful for a variety of applications, including optical power limiting and biomedical imaging.

1. Introduction

The phenomenon of two-photon absorption has received considerable attention since it was first predicted over 70 years ago.[1] Following initial demonstration of the effect,[2−4] a significant amount of research has been devoted to the development of novel structures that have large two-photon absorbing cross sections.[5−14] Recent work on two-photon absorbing systems has involved such diverse areas as photodynamic therapy (PDT),[15−17] optical power limiting (OPL),[18−22] two-photon fluorescence microscopy,[23−26] frequency up-converted lasing,[27−30] three-dimensional (3-D) optical data storage,[31−34] and 3-D microfabrication.[35,36]

The two-photon absorbing chromophore (TPAC), **1**, has been utilized in the study of novel materials, because of both its high two-photon absorbing cross section (6700 GM (±15%), where 1 GM = 10^{-50} cm^4 s)[37] and its functionalizable benzylic alcohol moiety. We have previously utilized **1** in an effort to develop molecules with increasingly large cross sections by incorporating it into the periphery of several dendritic structures.[38] The two-photon absorbing cross section of these molecules (**1**, **2**, and **3**) increased almost linearly between dendrimer generations, as did the single-photon absorption and emission properties, when measured at the same concentration. Further work involving fluorescence resonance energy transfer (FRET) between two multiphoton absorbing dyes has been performed utilizing a derivative of **1**.[39] We have recently combined **1** with the nile red derivative **4**[40] (which, along with model compound **5**, has a two-photon absorption cross section of only 750 GM) into a novel bichromophoric system (**6**).[41] This system undergoes near-quantitative FRET (~99%) from the two-photon absorbing chromophore at the periphery to the nile red moiety at the core when excited at either 405 nm (single-photon absorption) or 815 nm (two-photon absorption). Utilizing a two-photon absorbing antenna in combination with efficient FRET in this manner provides an effective method by which IR radiation can be used to activate other useful molecules designed for a specific application that absorb in the UV or visible regions but have little or no two-photon absorbing cross section in the IR region.

Given the extremely efficient FRET observed on both single- and two-photon excitation of **6**, these studies have been extended to the generation 1 (G-1) and generation 2 (G-2) dendritic systems (**7** and **8**, respectively). These systems contain a single nile red core and two or four peripheral TPAC moieties (which act as antennae), respectively. In addition, we have combined the nile red core with the TPAC **9**[42] to form a second G-1 dendritic energy transfer system (**10**). This system may prove very proficient in regard to harvesting the IR energy (by absorption and subsequent energy transfer) required for applications such as PDT and OPL, because **9** has a much higher TPA cross section than **1** (15 600 GM vs 6700 GM). In addition, the results obtained from the photophysical study of this dendrimer impose a higher degree of confidence in the idea

† Part of the special issue "Alvin L. Kwiram Festschrift".

* Author to whom correspondence should be addressed. Telephone: 510-643-3077. Fax: 510-643-3079. E-mail address: frechet@cchem.berkeley.edu.

10.1021/jp049948w CCC: $27.50
Published on Web 04/28/2004

CHART 1: Structures of TPAC Chromophores 1, 2, 3, 4, 5, and 9

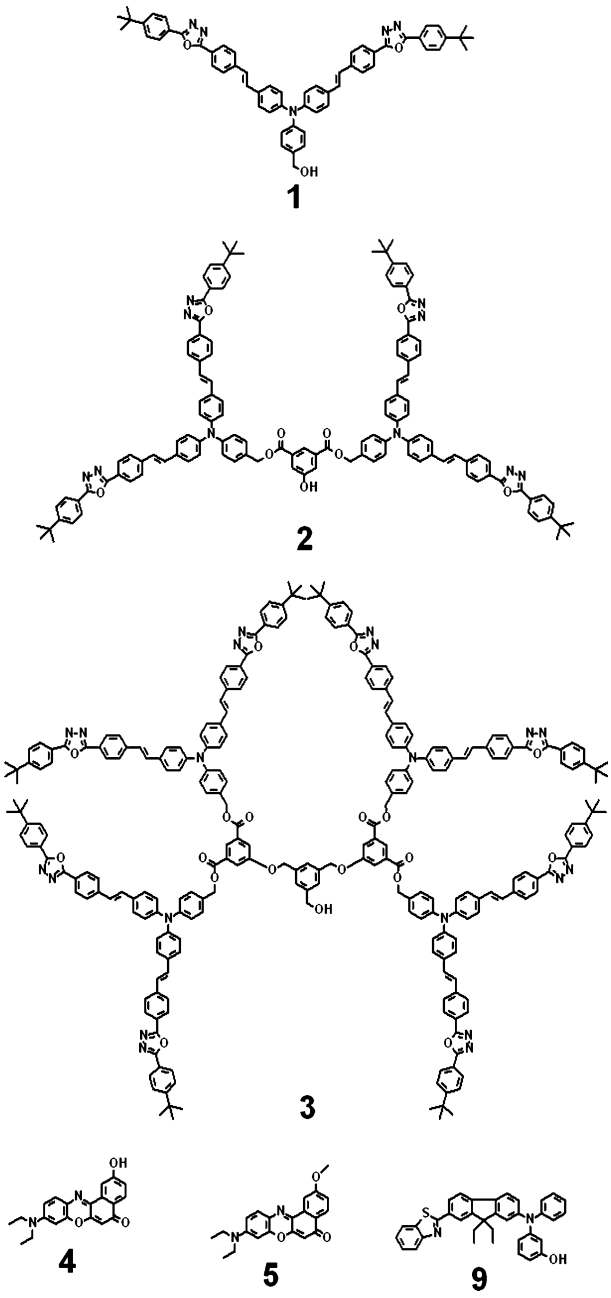

CHART 2: Structures of TPAC Chromophores 6, 7, 8, and 10

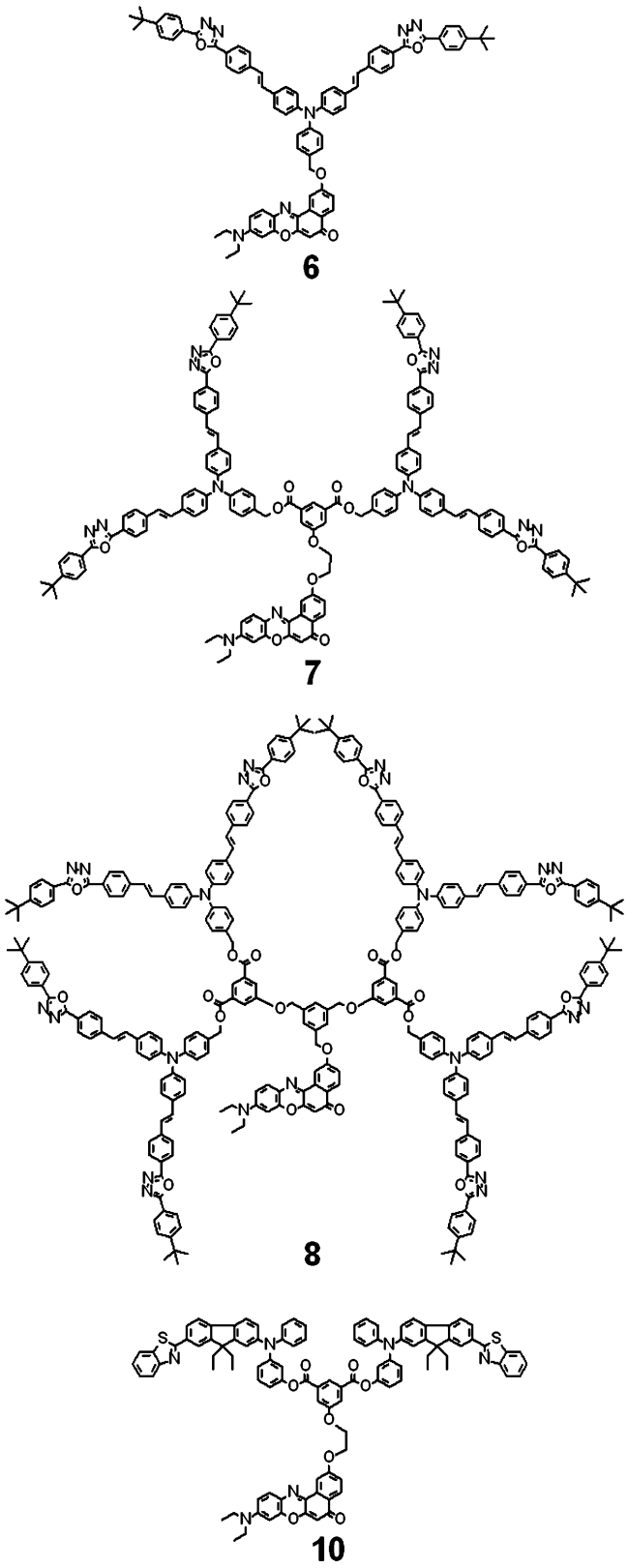

that this phenomenon of multiphoton absorption by an antenna, and activation of a separate chromophore through energy transfer, can be extended to multiple light-harvesting chromophores.

All these systems display efficient FRET and significant antenna effects on excitation with either UV or high-intensity IR radiation. A more-detailed explanation of the mechanism of energy transfer in **6**, **7**, and **8**, including their fluorescence lifetimes, has been described elsewhere.[43] The current work details both the synthesis of these dendritic energy-harvesting systems and the results of the relevant absorption, single-photon, and multiphoton fluorescence experiments.

2. Experimental Section

2.1. General. ^{1}H NMR spectra were recorded on either a Bruker AM 400 (400 MHz) or a Bruker DRX 500 (500 MHz) instrument. Anhydrous tetrahydrofuran (THF) was obtained by distillation over sodium using benzophenone as an indicator. Dry dimethylformamide (DMF) was purchased from Aldrich. Both low- and high-resolution mass spectra (HRMS) were obtained on a Micromass ProSpec system, using fast atom bombardment (FAB). Matrix-assisted laser desorption ionization time-of-flight (MALDI-TOF) mass spectrometry was performed

on a Perseptive Biosystems Voyager-DE spectrometer with an acceleration voltage of 20 keV, using α-hydroxycyanocinnamic acid as the matrix. Synthesis of the TPAC model compounds **1**−**3**,[38] the nile red derivative **4**,[40] the U.S. Air Force TPAC **9**,[42] and the parent model and target compounds (**5** and **6**, respectively)[41] have previously been reported. All solvents used for absorption and fluorescence measurements were spectroscopic-grade and were purged with N_2 for 10 min prior to taking measurements. UV−Vis measurements were conducted using a Varian Cary 50 spectrometer. Fluorescence measurements were taken on an ISA/SPEX Fluorolog 3.22 spectrometer that was equipped with double excitation and emission monochromators, a 450-W xenon lamp, and a digital photon counting photomultiplier. Fluorescence experiments were conducted in either 1.7×10^{-6} or 1.7×10^{-7} M solutions. All compounds were purified by preparatory thin-layer chromatography (TLC) immediately prior to photophysical analysis. To determine the relative quantum yields of the model and target compounds relative to each other, the absorbance of the model compounds was matched to the absorbance of the respective target at 390 nm (for TPAC model **9**), 405 nm (for TPAC models **1**, **2**, and **3**) or 540 nm (nile red models).

Antenna effects for the target compounds in **6**, **7**, **8**, and **10** are calculated by dividing the area of emission (centered at 595 nm) from the nile red core upon excitation of the two-photon absorbing moiety at 405 nm (or 390 nm for **10**) by the area of emission from direct excitation of the nile red moiety at 540 nm.

Energy transfer efficiencies[44,45] were calculated according to

$$\text{energy transfer efficiency (\%)} = \left(1 - \frac{\text{Abs.}_{\text{I}}(405\text{ nm})F_{\text{I}}}{\text{Abs.}_{\text{II}}(405\text{ nm})F_{\text{II}}}\right) \times 100$$

where Abs._{I} and Abs._{II} are the absorbances of the target (I) and model (II) compounds at the excitation wavelength (405 nm). This term becomes 1, as the absorbances were matched. $F_{\mathbf{I}}$ and $F_{\mathbf{II}}$ are the areas of emission from I and II.

The two-photon excitation studies were performed using a pulsed frequency-doubled Nd:YAG laser-pumped dye laser system (815 nm, pulse width of 8 ns, divergence angle of 1 mrad, beam size of ∼3 mm, and repetition rate of 10 Hz). The three-photon excitation studies utilized ∼1.3-μm ultrashort IR pulses from an optical parametric generator, which was pumped by laser pulses (∼790 nm and ∼150 fs) from a Ti:sapphire laser oscillator/amplifier system (model CPA2010, from Clark-MXR). The two- and three-photon induced fluorescence spectra of **5** (nile red), **9** (the second AF dye), and **10** (0.001 M solutions in THF) were measured in a 1-mm-path-length cell using a Holo Spec spectrometer from Kaiser, Inc.

2.2. 1,3,5-Tris(hydroxymethyl)benzene. Trimethyl-1,3,5-benzenetricarboxylate (4 g, 15.8 mmol, from Aldrich) in 25 mL THF was added through a dropping funnel into a 250-mL flask containing $LiAlH_4$ (1.8 g, 47.4 mmol) in 75 mL of dry THF at 0 °C under a N_2 atmosphere. After the mixture was stirred for 2 h, the reaction was quenched by the slow addition of a 1:1 mixture of Celite and $NaHSO_4 \cdot 7H_2O$. The suspension was filtered, and the Celite was washed twice with 100 mL of methanol (CH_3OH). Following removal of the solvent, the desired product was obtained in 95% yield (2.54 g). ^{1}H NMR of the product matched that of the authentic material:[46] ^{1}H NMR: (400 MHz, D_2O); δ 7.18 (s, 3H), 4.50 (s, 6H).

2.3. 1,3,5-Tris(bromomethyl)benzene. PBr_3 (6.1 mL, 64 mmol) was added dropwise to a suspension of 1,3,5-tris-(hydroxymethyl)benzene (2.7 g, 16.1 mmol) in 100 mL of dry diethyl ether in a 250-mL flask under a N_2 atmosphere at 0 °C. The solution was stirred at 0 °C for 2 h and then for an additional 6 h at room temperature. The reaction was quenched by pouring the solution onto ice, and then it was extracted three times with 100 mL of diethyl ether. The organic fractions were combined, dried with $MgSO_4$, filtered, and concentrated to give the desired product in an 80% yield (4.6 g). ^{1}H NMR of this material matched that of the known compound:[46] ^{1}H NMR: (400 MHz, $CDCl_3$) δ 7.34 (s, 3H), 4.45 (s, 6H).

2.4. Nile Red Bromide (11). To a 5-mL-capacity vial containing **4** (150 mg, 0.45 mmol) and K_2CO_3 (372 mg, 2.3 mmol) in 2 mL of dry DMF was added 1.16 mL (13.5 mmol, 20 eq.) of dibromoethane. The system was purged with N_2, heated to 65 °C, and allowed to stir for 18 h. Following extraction twice into 50 mL of CH_2Cl_2, drying with $MgSO_4$, removal of the solvent, and silica gel column chromatography (1:1 hexanes:EtOAc), the desired material was isolated in 90% yield (178 mg): ^{1}H NMR: (400 MHz, $CDCl_3$) δ 8.23 (d, 1H, 8.7 Hz), 8.05 (d, 1H, J = 2.6 Hz), 7.60 (d, 1H, J = 9.1 Hz), 7.19 (dd, 1H, J = 8.7, 2.6 Hz), 6.66 (dd, 1H, J = 9.1, 2.7 Hz), 6.46 (d, 1H, J = 2.7 Hz), 6.31 (s, 1H), 4.51 (t, 2 H, J = 6.2 Hz), 3.74 (t, 2H, J = 6.2 Hz), 3.47 (q, 4H, J = 7.1 Hz), 1.27 (t, 6H, J = 7.1 Hz); ^{13}C NMR: (100 MHz, $CDCl_3$) δ 183.01, 160.59, 152.01, 150.71, 146.79, 139.63, 133.99, 131.00, 127.84, 126.08, 124.61, 118.23, 109.48, 106.57, 105.21, 96.19, 67.94, 44.99, 28.82, 12.52; MS (FAB) m/z 441 (M^+); HRMS (FAB) Anal. Calcd. for $C_{22}H_{21}BrN_2O_3$: 441.081379. Found: 441.081090.

2.5. G-1 Model (12). Dry DMF (1.5 mL) was added to a 5-mL-capacity flask containing **11** (43 mg, 0.1 mmol), dimethyl-5-hydroxyisophthalate (41 mg, 0.2 mmol, from Aldrich), dry K_2CO_3 (120 mg, 0.4 mmol), and KI (5 mg, 0.04 mmol) under a N_2 atmosphere. The mixture was stirred at 60 °C for 16 h before being cooled, washed with NH_4Cl (saturated), extracted into CH_2Cl_2, dried with $MgSO_4$, and concentrated. The desired product was isolated in 81% yield (46 mg), following silica gel column chromatography (1:1 hexanes/EtOAc). ^{1}H NMR: (400 MHz, $CDCl_3$) δ 8.30 (s, 1H), 8.20 (d, 1H, J = 8.7 Hz), 8.05 (d, 1H, J = 2.5 Hz), 7.83 (s, 2H), 7.54 (d, 1H, J = 9.1 Hz), 7.19 (dd, 1H, J = 8.7, 2.6 Hz), 6.61 (dd, 1H, J = 9.1, 2.6 Hz), 6.40 (d, 1H, J = 2.6 Hz), 6.26 (s, 1H), 4.48−4.55 (m, 4H), 3.93 (s, 6H), 3.44 (q, 4H, J = 7.1 Hz), 1.25 (t, 6H, J = 7.1 Hz). ^{13}C NMR: (100 MHz, $CDCl_3$) δ 182.99, 165.91, 160.93, 158.57, 151.92, 150.66, 146.69, 139.54, 133.93, 131.74, 130.97, 127.69, 125.91, 124.57, 123.33, 119.87, 118.34, 109.45, 106.36, 105.11, 96.11, 66.95, 66.56, 52.35, 44.97, 12.53; MS (FAB) m/z 571 (M+H). HRMS (FAB) Anal. Calcd. for $C_{32}H_{30}N_2O_8$: 570.200216. Found: 570.201290.

2.6. G-1 Target (7). To a 5-mL-capacity vial containing 2 mL of dry DMF was added **11** (46 mg, 0.104 mmol), **2** (100 mg, 0.052 mmol), dry K_2CO_3 (35 mg, 0.21 mmol), and 18-crown-6 (5.5 mg, 0.02 mmol). The system was purged with N_2 and then stirred at 55 °C for 5 days before being washed with NH_4Cl (saturated), extracted into CH_2Cl_2, dried with $MgSO_4$, and concentrated. The product was isolated (38 mg, 32%), following several purifications by preparatory TLCs (twice with 98:2 CH_2Cl_2:CH_3OH, once with hexanes:EtOAc, and once with 98:2 CH_2Cl_2:CH_3OH). ^{1}H NMR: (400 MHz, $CDCl_3$) δ 8.43 (s, 1H), 8.26 (d, 1H, J = 8.7 Hz), 8.14 (d, 1H, J = 2.7 Hz), 8.04−8.11 (m, 16H), 7.93 (d, 2H, J = 1.4 Hz), 7.60 (d, 8H, J = 8.5 Hz), 7.54 (d, 8H, J = 8.6 Hz), 7.38−7.44 (m, 12H), 7.23 (dd, 1H, J = 8.7, 2.6 Hz), 6.99−7.19 (m, 20H), 6.65 (dd, 1H, J = 9.2, 2.7 Hz), 6.45 (d, 1H, J = 2.6 Hz), 6.32 (s, 1H), 5.36 (s, 4H), 4.5−4.65 (m, 4H), 3.45 (q, 4H, J = 7.0 Hz), 1.38 (s,

36H), 1.24 (t, 6H, 7.1 Hz). ^{13}C NMR: (100 MHz, $CDCl_3$) δ 183.07, 165.47, 164.48, 164.21, 161.02, 158.73, 155.24, 152.06, 150.76, 147.07, 146.86, 140.69, 139.78, 134.07, 131.94, 131.58, 131.02, 130.48, 130.11, 129.87, 127.89, 127.78, 127.15, 126.73, 126.70, 126.10, 125.98, 124.67, 124.57, 124.08, 122.41, 121.06, 120.25, 118.47, 109.51, 105.30, 96.27, 66.94, 66.68, 45.02, 35.05, 31.07, 12.55. MS (MALDI) *m*/*z* 2268, 2291 (M+Na).

2.7. Nile Red Diol (14). In a 10-mL-capacity flask containing 4 mL of dry THF was combined **4** (294 mg, 0,88 mmol), 1,3,5-tris(hydroxymethyl)benzene (140 mg, 0.88 mmol), and PPh_3 (230 mg, 0.88 mmol). After the system was cooled to 0 °C and the flask was purged with N_2, diethylazodicarboxylate (DEAD, 138 μL, 0.88 mmol) was added via syringe. The reaction mixture was stirred for 3 h before being washed with NH_4Cl, extracted into CH_2Cl_2, dried with $MgSO_4$, and concentrated. Following silica gel column chromatography, the product was isolated in 78% yield (334 mg). ^{1}H NMR: (400 MHz, dimethylsulfoxide (DMSO)-d_6) δ 7.99−8.02 (m, 2H), 7.56 (d, 1H, J = 9.1 Hz), 7.33 (s, 2H), 7.29 (dd, 1H, J = 8.7, 2.6 Hz), 7.25 (s, 1H), 6.77 (dd, 1H, J = 9.2, 2.6 Hz), 7.58 (d, 1H, J = 2.6 Hz), 6.14 (s, 1H), 5.26 (s, 2H), 4.52 (s, 4H), 3.46 (q, 4H, J = 6.9 Hz), 1.14 (t, 6H, J = 6.9 Hz). HH ^{13}C NMR: (100 MHz, DMSO-d_6) δ 181.32, 160.94, 151.67, 150.78, 146.40, 142.66, 140.76, 138.15, 136.07, 133.51, 130.90, 127.19, 125.00, 124.15, 123.90, 117.98, 110.03, 106.85, 104.04, 95.93, 69.83, 62.80, 44.41, 12.43. MS (FAB) *m*/*z* 485 (M+H). HRMS (FAB) Anal. Calcd. for $C_{29}H_{29}N_2O_5$: 485.207540. Found: 485.207647.

2.8. Nile Red Dibromide (15). Dry DMF was added via syringe to a mixture of **4** (100 mg, 0.3 mmol), 1,3,5-tris-(bromomethyl)benzene (1 g, 2.8 mmol, 10 eq), and NaH (11 mg, 0.45 mmol) in a 5-mL-capacity flask under a N_2 atmosphere. The solution was stirred for 45 min before being quenched with NH_4Cl (saturated), extracted into CH_2Cl_2, dried with $MgSO_4$, and concentrated. The desired product was isolated in 55% yield (47 mg) after silica gel column chromatography (1:1 hexanes:EtOAc). ^{1}H NMR: (400 MHz, $CDCl_3$) δ 8.25 (d, 1H, J = 8.8 Hz), 8.14 (d, 1H, J = 2.4 Hz), 7.61 (d, 1H, 9.1 Hz), 7.49 (s, 2H), 7.41 (s, 1H), 7.25 (dd, 1H, J = 8.8, 2.4 Hz), 6.67 (dd, 1H, J = 6.4, 2.4 Hz), 6.46 (d, 1H, J = 2.4 Hz), 6.31 (s, 1H), 5.24 (s, 2H), 4.51 (s, 4H), 3.48 (q, 4H, J = 7.1 Hz), 1.27 (t, 6H, J = 7.1 Hz). ^{13}C NMR: (100 MHz, $CDCl_3$) δ 183.07, 160.97, 152.03, 150.71, 146.82, 139.76, 138.78, 137.86, 134.02, 131.02, 129.22, 128.04, 127.84, 125.99, 124.63, 118.31, 109.48, 106.88, 105.24, 96.22, 69.37, 44.99, 32.62, 12.52. MS (FAB) *m*/*z* 611 (M+H); HRMS (FAB) Anal Calcd. for $C_{29}H_{26}Br_2N_2O_3$: 608.031015. Found: 608.029600.

2.9. G-2 Model (13). To 2 mL of dry THF in a 5-mL-capacity flask was added **14** (50 mg, 0.1 mmol), dimethyl-5-hydroxy-isophthalate (65 mg, 0.3 mmol, from Aldrich), and PPh_3 (80 mg, 0.3 mmol). After the flask was purged with N_2 and cooled to 0 °C, DEAD (48 μL, 0.3 mmol) was added via syringe. The solution was stirred for 1 h before being poured into 15 mL of NH_4Cl (saturated), extracted into CH_2Cl_2, dried with $MgSO_4$, and concentrated. Following silica gel column chromatography (1:1 hexanes:EtOAc), the desired product was obtained in 68% yield (60 mg). ^{1}H NMR: (500 MHz, $CDCl_3$) δ 8.31 (s, 2H), 8.25 (d, 1H, J = 8.7 Hz), 8.18 (d, 1H, J = 2.5 Hz), 7.86 (s, 4H), 7.58−7.6 (m, 3H), 7.54 (s, 1H), 7.27 (dd, 1H, J = 8.7, 2.6 Hz), 6.64 (dd, 1H, J = 8.7, 2.5 Hz), 6.47 (d, 1H, J = 3.0), 6.32 (s, 1H), 5.33 (s, 2H), 5.21 (s, 4H), 3.94 (s, 12H), 3.48 (q, 4H, J = 7.2 Hz), 1.27 (t, 6H, J = 7.2 Hz). ^{13}C NMR: (100 MHz, $CDCl_3$) δ 183.05, 165.90, 161.03, 158.50, 151.97, 150.69, 146.75, 139.61, 137.52, 137.08, 133.97, 131.75, 130.99, 127.75, 126.30, 126.04, 125.84, 124.62, 123.27, 119.97, 118.34, 109.49, 106.85, 105.14, 96.14, 69.90, 69.68, 52.35, 44.97, 12.92. MS (FAB) *m*/*z* 869 (M+H); HRMS (FAB) Anal. Calcd. for $C_{49}H_{44}N_2O_{13}$: 869.292165. Found: 869.292000.

2.10. G-2 Target (8). To **15** (19 mg, 0.03 mmol) in a 5-mL-capacity vial was added **2** (130 mg, 0.068 mmol), dry K_2CO_3 (90 mg, 0.24 mmol), 18-crown-6 (7 mg, 0.012 mmol), and 2 mL of acetone. The system was purged with N_2 and then stirred for 4 days at 50 °C before being washed with NH_4Cl (saturated), extracted into CH_2Cl_2, dried with $MgSO_4$, and concentrated. The product was isolated (53 mg, 41%) following several purifications by preparatory TLC procedures (twice with 98:2 CH_2Cl_2:CH_3OH, once with hexanes:EtOAc, and once with 98:2 CH_2Cl_2:CH_3OH). ^{1}H NMR: (500 MHz, $CDCl_3$) δ 8.40 (s, 2H), 8.20 (d, 1H, J = 8.5 Hz), 8.16 (d, 1H, J = 2.5 Hz), 8.02−8.05 (m, 32 H), 7.91 (d, 4H, J = 1.5 Hz), 7.60 (s, 2H), 7.56 (d, 16H, J = 8.5 Hz), 7.53 (d, 16H, J = 8.5 Hz), 7.35−7.40 (m, 24H), 7.21 (dd, 1H, J = 8.5, 2.5 Hz), 7.1−7.14 (m, 16H), 7.07 (d, 16H, J = 8.5 Hz), 6.97 (d, 8H, J = 16.0 Hz), 6.56 (dd, 1H, J = 8.5, 2.5 Hz), 6.35 (d, 1H, J = 2.5 Hz), 6.26 (s, 1H), 5.34 (s, 8H), 5.29 (s, 2H), 5.24 (s, 4H), 3.37 (q, 4H, J = 7.0 Hz), 1.36 (s, 72H), 1.19 (t, 6H, J = 7.0 Hz). ^{13}C NMR: (100 MHz, $CDCl_3$) δ 183.05, 165.33, 164.39, 164.11, 160.96, 158.50, 155.18, 151.93, 150.62, 147.16, 146.96, 146.70, 140.58, 137.13, 134.01, 131.89, 131.51, 130.99, 130.39, 129.99, 129.75, 127.75, 127.74, 127.07, 126.67, 126.63, 126.02, 125.93, 124.56, 124.46, 124.00, 123.43, 122.32, 120.97, 120.29, 119.97, 70.01, 66.84, 44.91, 34.98, 31.03, 12.50. MS (MALDI) *m*/*z* 4261.

2.11. $(TPAC)_2$−G-1−NR Target (10). To **9** (500 mg, 0.93 mmol), 5-(*tert*-butyldiphenylsilyl)hydroxyisophthalate (151 mg, 0.51 mmol), 1-(3dimethylaminopropyl)-3-ethylcarbodiimide hydrochloride (EDC) (195 mg, 1.02 mmol), DMAP (11.3 mg, 0.09 mol), and 4-(dimethylamino)-pyridinium-*p*-toluenesulfonate (DPTS) (55 mg, 0.19 mmol) was added 30 mL of freshly distilled CH_2Cl_2. The solution was stirred overnight at room temperature under N_2 and was then extracted into CH_2Cl_2 from aqueous NH_4Cl twice. The combined organic layers were dried with Na_2SO_4 and concentrated. The yellow residue (**16**) was used without further purification.

To a vial containing **16** (109 mg, 0.09 mmol), **11** (47 mg, 0.11 mmol), K_2CO_3 (25 mg, 0.18 mmol), and KI (3 mg, 0.02 mmol) under N_2 was added 2 mL of dry DMF. The system was further purged with N_2, heated to 60 °C, and stirred for 18 h. Following extraction twice into 50 mL of CH_2Cl_2, drying with Na_2SO_4, removal of the solvent, and silica gel column chromatography using a solvent gradient (3:2 hexanes:EtOAc to 1:1 hexanes:EtOAc), the desired material was isolated in a final yield of 37% over three steps (52 mg). ^{1}H NMR: (400 MHz, $CDCl_3$) δ = 8.54 (s, 1H), 8.24 (d, 1H, J = 9 Hz), 8.09 (m, 6H), 8.01 (d, 2H, J = 9 Hz), 7.98 (s, 2H), 7.91 (d, 2H, J = 8 Hz), 7.70 (d, 2H, J = 8 Hz), 7.63 (d, 2H, J = 8 Hz), 7.60 (d, 1H, J = 9 Hz), 7.49 (t, 2H, J = 8 Hz), 7.38 (t, 2H, J = 8 Hz), 7.3 (m, 6H), 7.09 (m, 4H), 7.20 (m, 6H), 7.02 (d, 2H, J = 8 Hz), 6.96 (t, 2H, J = 2 Hz), 6.85 (d, 2H, J = 8 Hz), 6.67 (m, 1H), 6.47 (d, 1H, J = 3 Hz), 6.33 (s, 1H), 4.58 (br s, 2H), 4.52 (br s, 2H), 3.48 (m, 4H), 2.08 (m, 4H), 1.97 (m, 4H), 0.88 (m, 6H), 0.36 (t, 12H, J = 7 Hz). MS (FAB) *m*/*z* = 1583.6 ($M+H^+$); found: 1584; HR MALDI Anal. Calcd. for $C_{102}H_{83}N_6O_8S_2$ ($M+H^+$): 1583.57. Found: 1583.15.

3. Results and Discussion

3.1. Synthesis. Synthesis of the parent two-photon absorbing chromophores **1**[37] and **9**,[42] the G-1 and G-2 two-photon absorbing model compounds (**2** and **3**),[38] and the parent target

and nile red model compounds (**5** and **6**, respectively)[41] have been previously reported. Coupling of **4** and dibromoethane to give the nile red functionalized bromide **11** was performed in acetone using K_2CO_3 (Scheme 1). Formation of the G-1 model compound **12** was accomplished in 81% yield by coupling **11** to dimethyl-5-hydroxyisophthalate using K_2CO_3 and KI in DMF at 65 °C for 16 h. The G-1 target compound **7** was synthesized in 32% yield by coupling **11** with **2** using the same reagents and stirring at 55 °C for 5 days (Scheme 1).

SCHEME 1

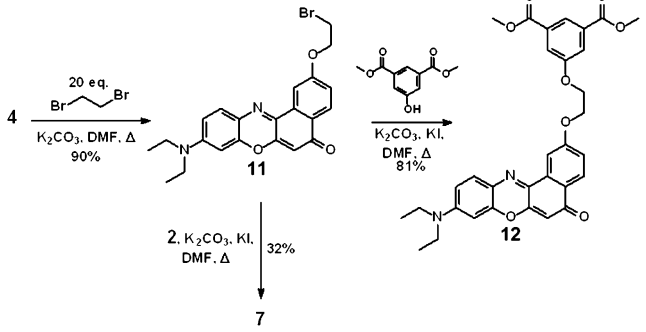

Scheme 2 illustrates the synthesis of the nile red containing dendritic building blocks (for the formation of the G-2 target and model compounds (**8** and **13**)), which began with the reduction of trimethyl-1,3,5-benzenetricarboxylate using $LiAlH_4$. The resulting 1,3,5-tris(hydroxymethyl)benzene was then reacted with 1 equiv of **4** under Mitsunobu conditions to yield the nile red functionalized diol **14**. Bromination of 1,3,5-tris(hydroxymethyl)benzene using PBr_3[46] gave 1,3,5-tris(bromomethyl)-benzene in 80% yield. This was then treated in DMF with 0.1 equiv of **4** in the presence of NaH to yield the nile red functionalized dibenzylbromide **15**.

SCHEME 2

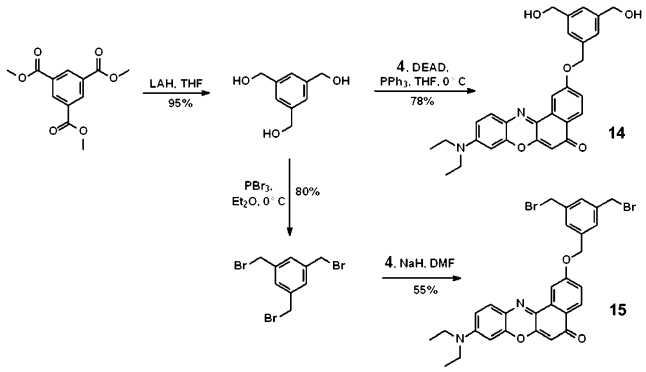

The G-2 model compound **13** was synthesized by reaction of **14** with dimethyl-5-hydroxyisophthalate using Mitsunobu conditions (Scheme 3). The target G-2 compound **8** was made by coupling **15** with **2**, in the presence of K_2CO_3 and 18-crown-6 in DMF (see Scheme 3). Coupling of the second two-photon absorbing chromophore (**9**) to a TBDPS protected diacid building block[38] utilizing 1-ethyl-3-(3-dimethylaminopropyl)-carbodiimide (EDC) yielded **16**, which was then coupled to **11** using K_2CO_3 and KI in dry DMF to give the G-1 target compound **10** (Scheme 4). All compounds were fully soluble in common organic solvents ($CHCl_3$, CH_2Cl_2, CH_3CN, and THF) and were characterized by ^1H and ^{13}C NMR, as well as mass spectrometry (MALDI-TOF or FAB).

3.2. Photophysical Characterization. *3.2.1. Absorbance.* The absorption spectra of the three bichromophoric target compounds

SCHEME 3

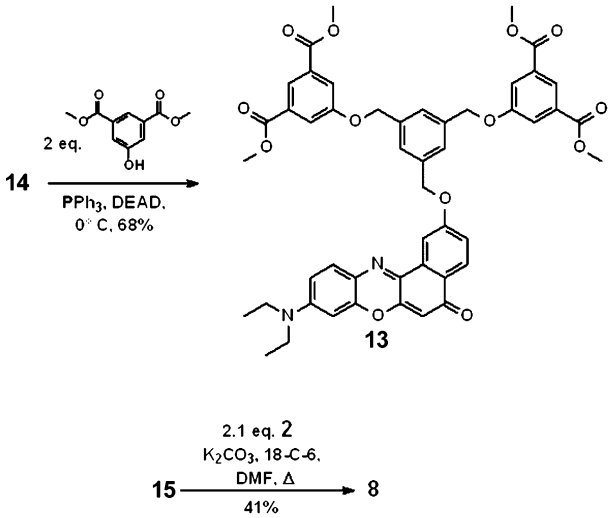

SCHEME 4

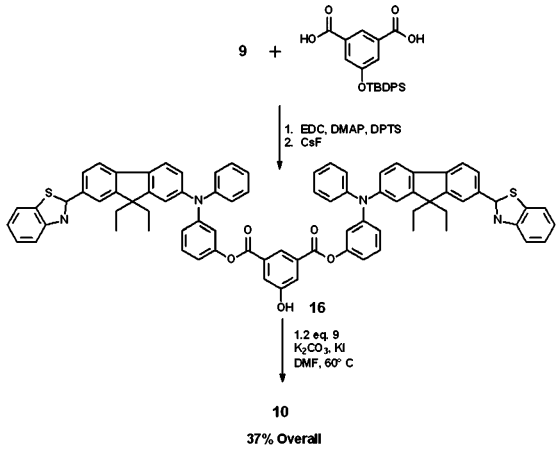

incorporating **1** (**6**, **7**, and **8**) in $CHCl_3$ at room temperature are presented in Figure 1a, which is normalized to 540 nm (the λ_{max} of the nile red chromophore). Each spectrum is a composite of the absorbances that result from the respective TPAC (**1**, **2**, and **3**) and nile red model compounds (**5**, **12**, and **13**; see inset in Figure 1). As expected, the area of absorbance attributable to the two-photon absorbing chromophore essentially doubles as the generation increases from **6** to **7** to **8**. This is identical to the previous result observed for **1**, **2**, and **3** in $CHCl_3$ when matched for concentration[38] and indicates that the molar absorptivity of the nile red moiety remains essentially the same between **6**, **7,** and **8**. The nile red model compounds (**5**, **12**, and **13**) all display identical absorption spectra above 300 nm in $CHCl_3$, where the aryl ether backbone of the dendrimer does not absorb. The absorption spectrum of **10**, the target system incorporating the second TPAC (**9**), is shown in Figure 1b, along with the respective TPAC and nile red model compounds **9** and **12**. As with the other target compounds, the absorption spectrum of **10** is a composite of two model compounds. Changing the solvent to THF has no significant effect on the shape, absorption maxima, or relative intensities ($<$10 nm shift) of any of the compounds.

3.2.2. Multiphoton Excitation Studies. Two-photon excitation with high-intensity IR laser radiation (815 nm, THF) on **6**, **7**, **8**, and **10** shows efficient energy transfer from the peripheral two-photon absorbing chromophores to the nile red core. This is evidenced by the attenuated fluorescence at 510 nm observed from equimolar solutions of the respective TPAC model

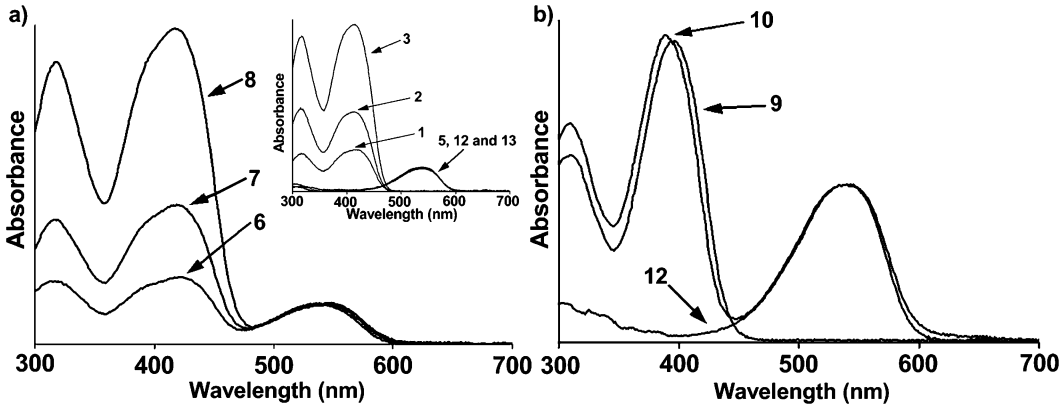

Figure 1. Absorbance spectra of the target and model compounds in $CHCl_3$ at room temperature. Panel a shows **6**, **7**, and **8** normalized to 540 nm, the absorbance maximum of the nile red moiety. The absorbance attributable to the TPAC chromophore essentially doubles with increasing generation. The absorption spectra of **6**, **7**, and **8** are composites of the respective model compounds. Inset shows TPAC models **1**, **2**, and **3** and nile red models **5**, **12**, and **13**, normalized to the absorption of **6**, **7**, and **8** at 405 and 540 nm, respectively. Panel b shows the absorbance spectra of the target compound **10** and respective model compounds **9** and **12** in $CHCl_3$ at room temperature. The absorption spectra of the model compounds **9** and **12** are normalized to the absorptions of **10** at 390 and 540 nm, respectively.

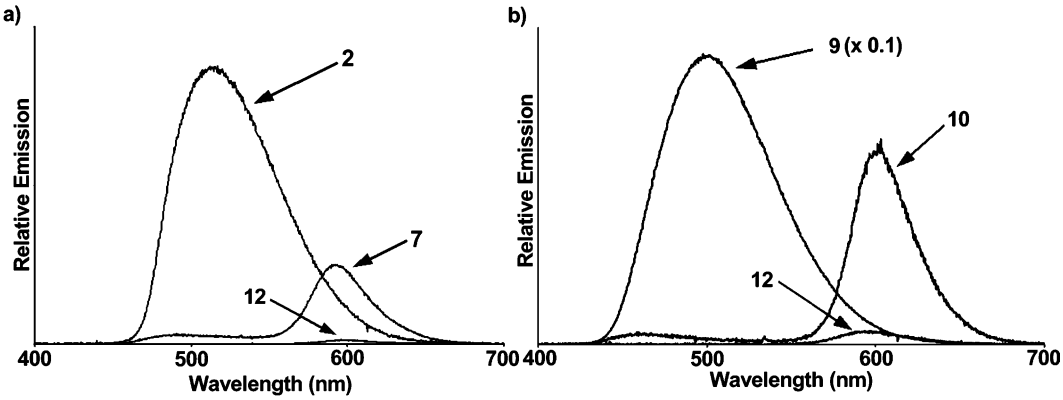

Figure 2. (a) Two-photon induced emission spectra of **2**, **7**, and **12** at room temperature in THF (0.001 M, λ_{ex} = 815 nm, 8-ns laser pulse). Emission at 510 nm from the TPAC moieties of **7** is significantly attenuated by energy transfer to the nile red chromophore, as compared to the emission from the TPAC model compound **2** when excited at the same wavelength. (b) Two-photon induced emission spectra of **9** (reduced 10-fold), **10**, and **12** at room temperature in THF (0.001 M, λ_{ex} = 815 nm, 8-ns laser pulse). As a result of energy transfer, the emission from the core nile red chromophore is increased 20-fold in **7** and 14-fold in **10**, compared to the excitation of **12**.

TABLE 1: Two-Photon Absorbing Cross-Section Values[a] for 5−8 and 10

compound	σ_2 ($\times 10^{-20}$ cm^4/GW)	GM
5	3	750
6	27	6700
7	48	11900
8	97	24100
10	13	3200

[a] All values ±15%.

compounds excited at the same wavelength. Figure 2a shows the luminescence for **7** and the model compounds **2** and **12**, and Figure 2b shows the luminescence for **10** and model compounds **9** and **12** after laser excitation. In addition, the emission from **6**, **7**, **8**, and **10** at 595 nm is increased by 8, 20, 34, and 14 times, respectively, from that of the appropriate nile red model compounds. As such, the majority of the emission observed from these molecules can be attributed to absorption and energy transfer from the two-photon absorbing chromophores. This "antenna effect" results from the much-larger two-photon absorbing cross section of the TPAC moieties at the excitation wavelength compared to the nile red core. The two-photon absorbing cross sections for **6**, **7**, **8**, **10** and the nile red model compound **5** are summarized in Table 1.

The intensity of the two-photon induced fluorescence signal showed a quadratic dependence on the input IR signal of ~815 nm, indicating that the emission from compounds **6**, **7**, **8**, and **10** was due to two-photon absorption.

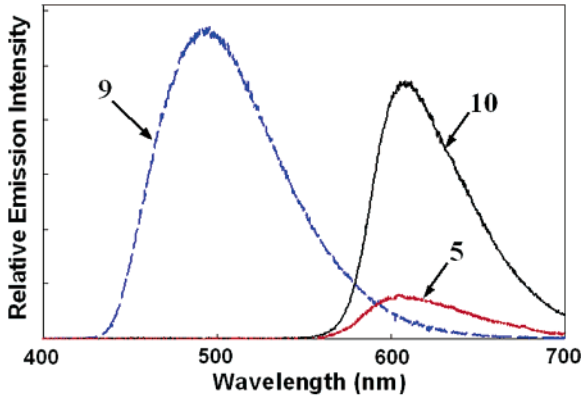

Figure 3. Three-photon induced fluorescence spectra of solutions of **9**, **10**, and **5** in THF (0.001 M, 1-mm path length) excited by a ~1.3-μm and ~150-fs laser pulse. Emission at 510 nm from compound **10** is significantly attenuated, compared to the emission from the TPAC model compound **9** when excited at the same wavelength. As a result of energy transfer, the emission from the core nile red chromophore in compound **10** is increased 4-fold, compared to excitation of compound **5** (nile red) at the same wavelength.

Figure 3 shows the three-photon absorption induced fluorescence spectral curves for solutions of compounds **5**, **9**, and **10**

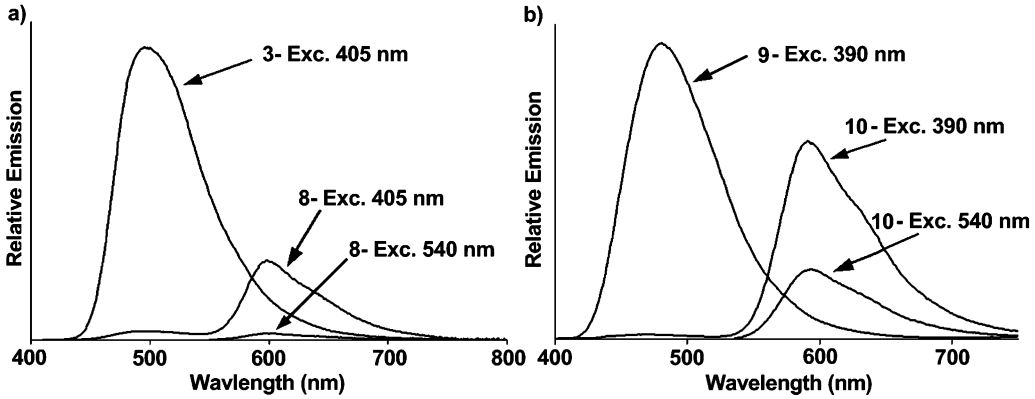

Figure 4. Emission spectra of **8** and **10** and their respective TPAC models **3** and **9**. Panel a shows single-photon emission spectra of **8** (λ_{ex} = 405 and 540 nm) and **3** (λ_{ex} = 405 nm), normalized for absorbance at 405 nm. Emission at 510 nm is quenched ~98% upon excitation of **8** at 405 nm, compared to that of **3** at the same wavelength. Irradiation of **8** at 405 nm shows a ~17-fold increase in core emission, compared to that at 540 nm. Panel b shows single-photon emission spectra of **10** (λ_{ex} = 390 and 540 nm) and **3** (λ_{ex} = 390 nm), normalized for absorbance at 390 nm. Emission at 490 nm is quenched ~98% upon excitation of **10** at 405 nm, compared to excitation of **9** at the same wavelength. Compared to excitation at 540 nm, when **10** is excited at 390 nm, an ~3-fold increase in core emission is observed.

in THF. These curves were obtained under the same excitation conditions of 1.3-μm laser pulses, using the same spectrometer as that used for the measurements shown in Figure 2. A more than 4-fold increase of the fluorescence emission at ~600-nm positions can be observed for compound **10** compared to compound **5**, indicating an obvious light-harvesting effect that is due to three-photon excitation. However, the apparent complete quenching of the ~510-nm emission band from the antenna compound **9** does not ensure a 100% radiationless energy transfer from the antenna to the core, because the possibility of reabsorption of this green emission propagating along the 1-mm path length inside the sample solution with relatively high concentration (0.001 M) cannot be neglected. Further measurement and studies are needed to separate specific contribution of real intermolecular (radiationless) energy transfer from the possible fluorescence−reabsorption process.

3.2.3. Single-Photon Emission Studies. The single-photon induced fluorescence properties of **1**−**3**, **5**−**10**, **12**, and **13** (all ~1.7×10^{-6} M solutions) were measured in both $CHCl_3$ and THF. To obtain relative fluorescence yields, the absorption spectra of the TPAC model compounds **1**, **2**, **3**, and **9** were matched to the absorption spectra of the respective bichromophoric compound **6**, **7**, **8**, or **10** at the wavelength for excitation of the TPAC moieties (405 nm for **6**, **7**, and **8**; 390 nm for **10**). Similarly, the absorptions of the nile red model compounds **5**, **12**, and **13** were matched to the absorption spectra of **6** and **10**, **7**, and **8**, respectively, at 540 nm, which is the wavelength used for selective excitation of the nile red moiety.

Irradiation of the TPAC model compounds **1**, **2**, **3**, and **9** at 540 nm with low-intensity light (not laser excitation) in both $CHCl_3$ and THF resulted in no observable fluorescence. Thus, any emission observed upon irradiation of **6**, **7**, and **8** at 540 nm can be attributed to direct excitation of the nile red core. Emission from the nile red model compounds **5**, **12**, and **13** in both solvents was attenuated by >90% upon excitation at the maximum absorption wavelength of the two-photon absorbing chromophores (390 or 405 nm), compared to excitation at 540 nm. This results from the significant difference in molar absorptivity of these compounds between the two wavelengths and indicates that the emission from the nile red core in **6**, **7**, **8**, and **10** is almost entirely attributable to energy transfer (vide infra) from the TPAC moieties, and not from direct excitation of the core. As expected, **5**, **12**, and **13** all display the same fluorescence (area and band shape) when excited at either 405 or 540 nm. This indicates that the dendritic backbone has no effect on the emission properties of the system. Excitation of **1**, **2**, and **3** in both $CHCl_3$[38] and THF (1.86×10^{-6} M) at 405 nm resulted in an almost doubling of the emission (λ_{max} = 510 nm), respectively, with increasing generation.

TABLE 2: Energy Transfer Efficiency and Relative Antenna Effects Observed on Single-Photon Excitation of 6−8 and 10 in $CHCl_3$ and THF

	energy transfer efficiency (%)		antenna effect[a]	
compound	$CHCl_3$	THF	$CHCl_3$	THF
6	>99	>99	3.4	4.5
7	>96	>98	7.1	8.2
8	>98	>98	17	17
10	>99	>98	2.9	2.8

[a] All values ±10%.

The single-photon induced emission spectra of **8** and the TPAC model compound **3** are presented in Figure 4a. Irradiation of **8** at 405 nm in $CHCl_3$ resulted in emission mainly from the nile red chromophore (595 nm), with only a small amount of emission (<2%) at 510 nm, compared to the irradiation of **3** at the same wavelength. This significant decrease in fluorescence from the TPAC moieties represents an almost-quantitative (98%) energy transfer[44,45] between the two chromophores. Similar energy transfer efficiencies are also observed for **6** and **7** (Table 2). The residual signal observed at 510 nm from both **7** and **8** results, at least partially, from a small amount of **1** present in solution, which likely results from the hydrolysis of the ester linkages in these compounds, rather than incomplete energy transfer. The identification of this impurity, which cannot be completely removed, even after several purifications, was based upon MALDI-TOF data, which shows the appearance of peaks at 1404 *m*/*z* (hydrolysis product: **7** minus **1**) for **7**, 3399 *m*/*z* (hydrolysis product: **8** minus **1**) for **8**, and 880 *m*/*z* (from **1**) for both **7** and **8**. Thus, the energy transfer efficiencies reported for **7** and **8** actually represent a minimum value. A 17-fold increase in core emission (antenna effect) is observed on excitation of **8** at 405 nm in $CHCl_3$, compared to direct excitation of the nile red core at 540 nm (Figure 4a), even though there is a net loss of energy that is due to the low quantum yield of fluorescence from the nile red core. This change in core emission is used to quantify the ability of the donor chromophores to act as antennae, by gathering light from a region of the spectrum different to that of the acceptor and concentrating it at the single acceptor chromophore. Because of the 6-fold relative difference in molar absorptivity of the

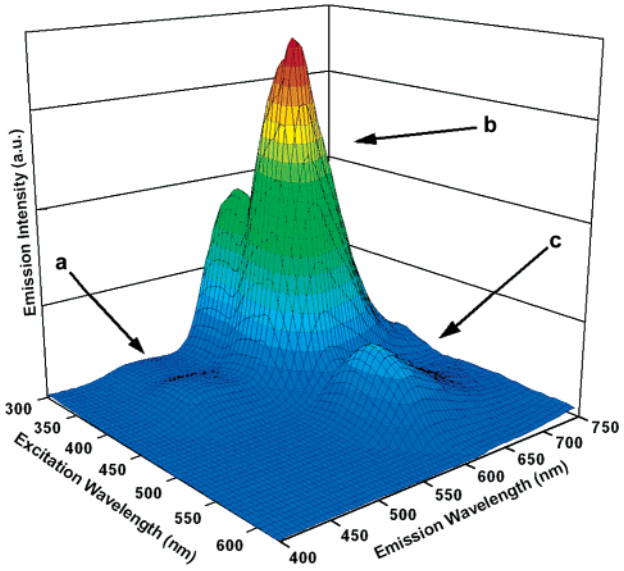

Figure 5. Total emission from **7** in $CHCl_3$ at room temperature: (a) residual emission from the TPAC moieties, (b) emission from the nile red core following excitation of the TPAC moieties and FRET, and (c) emission from the nile red core on direct excitation.

donor at 405 nm and the acceptor at 540 nm in **8**, we would expect to see a similar difference in the emission from the acceptor after excitation of **8** at these wavelengths. Thus, the antenna effect describes the overall increase in acceptor chromophore emission that is due to the presence of the donor chromophores and is independent of the physical processes occurring within the molecule, such as the microenvironment of the acceptor and the possible accompanying change in luminescence quantum yield, molar absorptivities, etc. Our confidence in the observed 17-fold increase, as opposed to the expected 6-fold increase, was solidified after performing the experiments several times and ensuring that the excitation intensity of the lamp was normalized at both wavelengths. An explanation of this observed discrepancy, and a more complete picture of the electronic interactions occurring within this system, can only begin with a more detailed study of the system using time-resolved methods. However, as expected, these antenna effects appear to approximately double with increasing generation between **6**, **7**, and **8**, as the number of two-photon absorbing chromophores doubles (see Table 2).

The emission spectra of **10** (at 390- and 540-nm excitation) and the respective TPAC model compound **9** (390-nm excitation) in THF are shown in Figure 4b. As with the other systems, an almost-quantitative energy transfer (>98%) is observed on excitation of **10** at 390 nm, compared to excitation of **9** at the same wavelength. Irradiation of **10** at 390 nm also results in a large antenna effect (an ~3-fold increase) in the core emission at 595 nm, compared to direct core excitation at 540 nm. The energy transfer efficiencies and antenna effects that result from excitation of **6**, **7**, **8**, and **10** in both $CHCl_3$ and THF are summarized in Table 2. Both solvents give similar results for all compounds.

The total emission spectrum of **7** is presented in Figure 5. This surface is resolved by exciting **7** at each wavelength from 300 nm to 650 nm and measuring the resulting emission spectrum from 400 nm to 750 nm. It provides an effective means of visualizing the steady-state photophysical properties of the energy transfer system. Residual emission from the peripheral two-photon absorbing dyes (Figure 5a) is negligible compared to the emission from the nile red core resulting from energy transfer (Figure 5b). The significant antenna effect in emission between excitation of **7** at the peripheral two-photon absorbing dyes (Figure 5b), compared to direct excitation at the nile red core (Figure 5c) is clearly visible.

3.3. Mechanism of Energy Transfer. The energy transfer process in these systems, following excitation of the two-photon absorbing chromophores by either single-photon or multiphoton excitation events, is believed to occur through a nonradiative, Förster-type mechanism (FRET).[43] Dexter-type (through bond) energy transfer has been discounted in similar systems[41,45,47−49] and is excluded here, because of the methylene spacers in the dendritic backbone. Radiative "trivial" energy transfer has also been eliminated as a possible mechanism in the single-photon work by repeating the emission experiments at a lower concentration ($\sim 1.7 \times 10^{-7}$ **M**). Excitation of **7** and **8** and their respective model compounds under these conditions resulted in the same energy transfer efficiencies and antenna effects as those observed at the higher concentration. If radiative energy transfer was occurring, the fluorescence from the TPAC chromophore should increase at these very low concentrations, where the acceptor moiety is not able to reabsorb as much of the emitted light.

Although reabsorption is not negligible, because of the high concentrations used in the multiphoton experiments, the possibility of a radiative energy transfer mechanism can be excluded by dynamic fluorescence measurements. For example, emission at ~595 nm from dendritic compound **8** displays a fast single-exponential decay with a 2.5 ns lifetime that is evidence of a nonradiative transfer mechanism. According to the convolution analysis, a nonexponential temporal behavior with a slow rise, followed by a much-slower decay process, would be observed, if radiative energy transfer was the major mechanism.[43]

4. Summary and Conclusions

Efficient single-photon and multiphoton induced fluorescence resonance energy transfer (FRET) (>96%) has been demonstrated between donor two-photon absorbing chromophore (TPAC) moieties and a nile red acceptor chromophore in the novel dendrimers **7**, **8**, and **10**. These systems allow for the spectral and spatial concentration of UV−visible and high-intensity IR radiation at a single chromophore located at the core of the dendrimer. The efficient energy transfer and "antenna effects" observed in these systems, coupled with the fact that they can efficiently absorb multiple photons, makes them potentially very useful. This strategy of using a light-harvesting "antenna" may be extended to activate different acceptors with a range of emission wavelengths or excited-state chemistry, provided that the energetics are appropriate for energy transfer. Several systems exploring these possibilities with specific applications, such as optical power limiting (OPL) and photodynamic therapy (PDT), are currently being investigated. In addition, we are investigating the use of different red- and green-emitting cores with higher emission quantum yields than nile red, which may prove useful in such areas as two-photon induced lasing and biomedical imaging.

Acknowledgment. Financial support of this work by the AFOSR-MURI program (under Grant No. F49620-96-1-0035), AFOSR-DURINT (under Grant No. F496200110358), and DOE-BES is acknowledged with thanks. D.W.B. thanks the Natural Sciences and Engineering Research Council (NSERC) of Canada for a postdoctoral fellowship. We thank Prof. A. Adronov (McMaster University), for providing a sample of **3**, and Mr. Dann Holmes, for his assistance in the synthesis of several compounds.

References and Notes

(1) Goppert-Mayer, M. *Ann. Phys. (Berlin)* **1931**, *9*, 273.
(2) Peticola, W. L. *Annu. Rev. Phys. Chem.* **1967**, *18*, 233.
(3) McClain, W. M. *Acc. Chem. Res.* **1974**, *7*, 129.
(4) Birge, R. R.; Pierce, B. M. *J. Chem. Phys.* **1979**, *70*, 165.
(5) Bhawalkar, J. D.; He, G. S.; Prasad, P. N. *Rep. Prog. Phys.* **1996**, *59*, 1041.
(6) He, G. S.; Yuan, L. X.; Cui, Y. P.; Li, M.; Prasad, P. N. *J. Appl. Phys.* **1997**, *81*, 2529.
(7) Kim, O. K.; Lee, K. S.; Woo, H. Y.; Kim, K. S.; He, G. S.; Swiatkiewicz, J.; Prasad, P. N. *Chem. Mater.* **2000**, *12*, 284.
(8) Zhou, Y. F.; Meng, F. Q.; Zhao, X.; Xu, D.; Jiang, M. H. *Solid State Commun.* **2000**, *116*, 605.
(9) Wang, X. M.; Wang, D.; Zhou, G. Y.; Yu, W.; Zhou, Y. T.; Fang, Q. F.; Jiang, M. H. *J. Mater. Chem.* **2001**, *11*, 1600.
(10) Drobizhev, M.; Karotki, A.; Rebane, A.; Spangler, C. W. *Opt. Lett.* **2001**, *26*, 1081.
(11) Pan, G. L.; Fan, M. G.; Fan, P.; Wang, H. Z.; Wei, Z. C. *Chem. Commun.* **2001**, 1744.
(12) Lee, W. H.; Lee, H.; Kim, J. A.; Choi, J. H.; Cho, M. H.; Jeon, S. J.; Cho, B. R. *J. Am. Chem. Soc.* **2001**, *123*, 10658.
(13) Reinhardt, B. A.; Brott, L. L.; Clarson, S. J.; Dillard, A. G.; Bhatt, J. C.; Kannan, R.; Yuan, L.; He, G. S.; Prasad, P. N. *Chem. Mater.* **1998**, *10*, 1863.
(14) Kannan, R.; He, G. S.; Yuan, L.; Xu, F.; Prasad, P. N.; Dombroskie, A. G.; Reinhardt, B. A.; Baur, J. W.; Vaia, R. A.; Tan, L.-S. *Chem. Mater.* **2001**, *13*, 1896.
(15) Bhawalkar, J. D.; Kumar, N. D.; Zhao, C. F.; Prasad, P. N. *J. Clin. Med. Surg.* **1997**, *37*, 510.
(16) Fisher, W. G.; Partridge, W. P.; Dees, C.; Wachter, E. A. *Photochem. Photobiol.* **1997**, *66*, 141.
(17) Frederiksen, P. K.; Jørgensen, M.; Ogilby, P. R. *J. Am. Chem. Soc.* **2001**, *123*, 1215.
(18) He, G. S.; Bhawalkar, J. D.; Prasad, P. N.; Reinhardt, B. A. *Opt. Lett.* **1995**, *20*, 1524.
(19) Joshi, M. P.; Swiatkiewicz, J.; Xu, F. M.; Prasad, P. N. *Opt. Lett.* **1998**, *23*, 1742.
(20) Spangler, C. W. *J. Mater. Chem.* **1999**, *9*, 2013.
(21) Lei, H.; Wang, H. Z.; Wei, Z. C.; Tang, X. J.; Wu, L. Z.; Tung, C. H.; Zhou, G. Y. *Chem. Phys. Lett.* **2001**, *333*, 387.
(22) Zhou, G. Y.; Wang, X. M.; Wang, D.; Shao, Z. S.; Jiang, M. H. *Appl. Opt.* **2002**, *41*, 1120.
(23) Denk, W.; Strickler, J. H.; Webb, W. W. *Science* **1990**, *248*, 73.
(24) Shen, Y. Z.; Jakubczyk, D.; Xu, F.; Swiatkiewicz, J.; Prasad, P. N.; Reinhardt, B. A. *Appl. Phys. Lett.* **2000**, *76*, 1.
(25) Belfield, K. D.; Schafer, K. J.; Mourad, W.; Reinhardt, B. A. *J. Org. Chem.* **2000**, *65*, 4475.
(26) So, P. T. C.; Dong, C. Y.; Masters, B. R.; Berland, K. M. *Annu. Rev. Biomed. Eng.* **2000**, *2*, 399.
(27) He, G. S.; Bhawalkar, J. D.; Zhao, C. F.; Park, C.-K.; Prasad, P. N. *Opt. Lett.* **1995**, *20*, 2393.
(28) Fakis, M.; Polyzos, J.; Tsigaridas, G.; Parthenios, J.; Fragos, A.; Giannetas, V.; Persephonis, P.; Mikroyannidis, J. *Chem. Phys. Lett.* **2000**, *323*, 111.
(29) Wang, C.; Wang, X.; Shao, Z.; Zhao, X.; Zhou, G.; Wang, D.; Fang, Q.; Jiang, M. *Opt. Commun.* **2001**, *192*, 315.
(30) Tang, X.-J.; Wu, L.-Z.; Zhang, L.-P.; Tung, C.-H. *Chem. Phys. Lett.* **2002**, *356*, 573.
(31) Parthenopolous, D. A.; Rentzepis, P. M. *Science* **1989**, *245*, 843.
(32) Pudavar, H. E.; Joshi, M. P.; Prasad, P. N.; Reinhardt, B. A. *Appl. Phys. Lett.* **1999**, *74*, 1338.
(33) Cumpston, B. H.; Ananthavel, S. P.; Barlow, S.; Dyer, D. L.; Ehrlich, J. E.; Erskine, L. L.; Heikal, A. A.; Kuebler, S. M.; Lee, I. Y. S.; McCord-Maughon, D.; Qin, J. Q.; Rockel, H.; Rumi, M.; Wu, X. L.; Marder, S. R.; Perry, J. W. *Nature* **1999**, *398*, 51.
(34) Belfield, K. D.; Liu, Y.; Negres, R. A.; Fan, M.; Pan, G.; Hagan, D. J.; Hernandez, F. E. *Chem. Mater.* **2002**, *14*, 3663.
(35) Zhou, W.; Kuebler, S. M.; Braun, K. L.; Yu, T.; Cammack, J. K.; Ober, C. K.; Perry, J. W.; Marder, S. R. *Science* **2002**, *296*, 1106.
(36) Ohkuma, S.; Yamashita, T. *J. Photopolym. Sci. Technol.* **2002**, *15*, 23.
(37) Chung, S.-J.; Kim, K.-S.; Lin, T.-C.; He, G. S.; Swiatkiewicz, J.; Prasad, P. N. *J. Phys. Chem. B* **1999**, *103*, 10741.
(38) Adronov, A.; Fréchet, J. M. J.; He, G. S.; Kim, K.-S.; Chung, S.-J.; Swiatkiewicz, J.; Prasad, P. N. *Chem. Mater.* **2000**, *12*, 2838.
(39) Chung, S.-J.; Lin, T.-C.; Kim, K.-S.; He, G. S.; Swiatkiewicz, J.; Prasad, P. N.; Baker, G. A.; Bright, F. V. *Chem. Mater.* **2001**, *13*, 4071.
(40) Briggs, M. S. J.; Bruce, I.; Miller, J. N.; Moody, C. J.; Simmonds, A. C.; Swann, E. *J. Chem. Soc., Perkin Trans. 1* **1997**, *7*, 1051.
(41) Brousmiche, D. W.; Serin, J. M.; Fréchet, J. M. J.; He, G. S.; Lin, T.-C.; Chung, S.-J.; Prasad, P. N. *J. Am. Chem. Soc.* **2003**, *125*, 1448.
(42) Tan, L.-S.; Kannan, R.; Matuszewski, M. J.; Khur, I. J.; Feld, W. A.; Dang, T. D.; Dombroskie, A. G.; Vaia, R. A.; Clarson, S. J.; He, G. S.; Lin, T.-C.; Prasad, P. N. *Proc. SPIE−Int. Soc. Opt. Eng.* **2003**, *4797*, 171.
(43) He, G. S.; Lin, T.-C.; Cui, Y.; Prasad, P. N.; Brousmiche, D. W.; Serin, J. M.; Frechet, J. M. J. *Opt. Lett.* **2003**, *28*, 768.
(44) Mugnier, J.; Pouget, J.; Bourson, J.; Valeur, B. *J. Lumin.* **1985**, *33*, 273.
(45) Adronov, A.; Gilat, S. L.; Frechet, J. M. J.; Ohta, K.; Neuwahl, F. V. R.; Fleming, G. R. *J. Am. Chem. Soc.* **2000**, *122*, 1175.
(46) Gil, L.; Han, Y.; Opas, E. E.; Rodan, G. A.; Ruel, R.; Seedor, J. G.; Tyler, P. C.; Young, R. N. *Bioorg. Med. Chem.* **1999**, *7*, 901.
(47) Gilat, S. L.; Adronov, A.; Frechet, J. M. J. *Angew. Chem., Int. Ed.* **1999**, *38*, 1422.
(48) Serin, J. M.; Brousmiche, D. W.; Frechet, J. M. J. *Chem. Commun.* **2002**, 2605.
(49) Serin, J. M.; Brousmiche, D. W.; Fréchet, J. M. J. *J. Am. Chem. Soc.* **2002**, *124*, 11848.